



UNIVERSITY OF LEEDS

This is a repository copy of *On-Demand Delivery of Single DNA Molecules Using Nanopipets*.

White Rose Research Online URL for this paper:
<http://eprints.whiterose.ac.uk/101070/>

Version: Accepted Version

Article:

Ivanov, AP, Actis, P orcid.org/0000-0002-7146-1854, Jonsson, P et al. (3 more authors) (2015) On-Demand Delivery of Single DNA Molecules Using Nanopipets. *ACS Nano*, 9 (4). pp. 3587-3595. ISSN 1936-0851

<https://doi.org/10.1021/acsnano.5b00911>

Reuse

Items deposited in White Rose Research Online are protected by copyright, with all rights reserved unless indicated otherwise. They may be downloaded and/or printed for private study, or other acts as permitted by national copyright laws. The publisher or other rights holders may allow further reproduction and re-use of the full text version. This is indicated by the licence information on the White Rose Research Online record for the item.

Takedown

If you consider content in White Rose Research Online to be in breach of UK law, please notify us by emailing eprints@whiterose.ac.uk including the URL of the record and the reason for the withdrawal request.



eprints@whiterose.ac.uk
<https://eprints.whiterose.ac.uk/>

On-demand delivery of single DNA molecules with nanopipets

Aleksandar P. Ivanov^{1,#} Paolo Actis^{2,#}, Peter Jönsson³, David Klenerman³, Yuri Korchev²,
Joshua B. Edel^{1,*}

1 Department of Chemistry, Imperial College London, SW7 2AZ, United Kingdom

2 Department of Medicine, Imperial College London, W12 0NN, United Kingdom

3 Department of Chemistry, University of Cambridge, CB2 1EW, United Kingdom

equal contribution

*corresponding author: joshua.edel@imperial.ac.uk

Keywords

Single-molecule delivery, label-free detection, nanopore, nanopipette, DNA

Rapid single-molecule detection and controllable single-molecule delivery are two of the central themes of modern nanotechnology. Unfortunately these themes are often disconnected, particularly in environments which require physiological and label-free conditions. A class of versatile single-molecules detectors - nanopores, has shown exceptional promise for label-free analysis of key life components such as DNA, RNA, and proteins,¹⁻⁶ but has not been used for the controllable delivery of biomolecular species, partially due to the stochastic (random) nature of the transport of analyte through the nanopore. Here, we address this limitation and report on simultaneous label-free detection and concentration independent (non-stochastic) on-demand delivery of single DNA molecules with nanopores, with precise control of the time of delivery and the number of delivered molecules. Molecular delivery is demonstrated down to picomolar concentrations ($<10^6$ DNA molecules in sub-microliter), advancing high-sensitivity detection and delivery of unamplified samples with nanopores. Additionally, molecules can be controllably transported back and forth to the nanopore by using asymmetric geometry and voltage pulses, acting as “on-off switch” for molecular delivery on-demand. We envision applications in controllable delivery of individual oligonucleotides (inside living cells), providing new insights in processes such as gene regulation and infection, and single-molecule PCR, to name a few.

In a typical nanopore label-free detection, two ionic reservoirs are connected via a nanoscale pore. Voltage is applied across the nanopore to generate a steady-state ionic current that depends on the pore dimensions, charge, and the ionic strength of the solution.^{1,3} Analytes are electrokinetically translocated through the nanopore and are detected by transient variations in the ionic current. A sub-class of nanopores, used in this work, is nanopipettes. Nowadays, nanopipettes are rapidly and inexpensively laser pulled from glass capillaries, resulting in a

sharp tip with a single nanopore, which can be used as single-molecule label-free sensors⁷⁻⁹, just like conventional solid-state nanopores. Because of their high-aspect ratio geometry and exceptionally sharp tips, nanopipettes offer an important advantage over conventional nanopores and can be used for single cell interrogation^{10,11} and as a macroscopic delivery vehicle for intracellular injection¹²⁻¹⁶. However, measurements of the concentration of delivered molecules have so far only been quantified only in the proximity of the tip by fluorescence^{16,13,17} and real-time quantitative delivery of individual molecules combined with label-free nanopore detection has yet not been achieved. In fact for label-free detection, nanopipettes are used exclusively as analytical platforms of molecules that have been transported from the outside reservoir to the inside of the nanopipette,^{8,9,18-21} without utilizing the advantages of using nanopipettes as a delivery vehicle of molecular species. We here show that it is also possible to label-free detect and deliver, molecules from the inside of the nanopipette in a precise manner, with single-molecule control.

A schematic of the principle behind the experiment is shown in Figure 1a,b. Quartz nanopipettes were fabricated by laser-assisted pulling as described in the Methods section. The nanopipettes used in this study had a resistance of $250 \pm 35 \text{ M}\Omega$ (in 0.1 M KCl, 10 mM Tris/EDTA, pH 8) and a nanopore diameter of $25 \pm 4 \text{ nm}$, as determined by SEM (Fig. 1c). All nanopipettes exhibited rectification, $I_{-500 \text{ mV}}/I_{500 \text{ mV}} = 1.64 \pm 0.40$ (Fig. 1d), consistent with the ion depletion and accumulation model described by Lan et. al for negatively charged conical geometries.²²

The nanopipettes were filled with (5 kbp or 10 kbp) double-stranded DNA solution and Ag/AgCl electrodes were fitted both in the nanopipette (working electrode) and in the external reservoir containing only buffer (ground/reference electrode). Under these conditions, the

negatively charged DNA molecules inside the nanopipette migrate toward the inner electrode under positive applied potentials and toward the nanopore under negative potentials. In contrast to traditional nanopore experiments where a constant DC voltage is applied, we used periodic cycles of positive (V^+) and negative (V^-) potential pulses with durations t^+ and t^- , respectively. This allowed us to minimize nanopore clogging and importantly to deliver individual molecules through the nanopore in a non-stochastic manner (Fig. 1a,b). We observed that in each cycle, the time between the application of the negative bias and the detection of the first translocation event (dT) was remarkably regular and could be controlled by varying the magnitude of V^- , V^+ and t^+ . Figure 2a shows representative time traces for voltage ($V-t$) and current ($I-t$) for 500 seconds (24 consecutive delivery cycles) for 150 pM, 10 kbp DNA. During a V^- pulse individual DNA molecules are delivered and detected as transient changes of the ionic current as shown in Fig. 2b. At 0.1 M KCl, the translocation of DNA through the nanopore elicits a temporary increase in the conductance rather than a decrease. This effect is due to conducting counter ions that shield the negatively charged phosphate backbone of the translocated DNA molecule, which has been observed before in similar ionic strength conditions.^{18,23} The high reproducibility in the measured current between each cycle can be used to combine single-molecule detection statistics from each cycle in all event histograms. Histograms and event scatter plots of peak current versus dwell time and equivalent charge (integrated current area per translocation) vs dwell time are shown in Fig. 2c indicating that the 10 kbp DNA is in an unfolded state when being translocated through the nanopore.⁸ At $V^- = -300$ mV the most probable nanopore dwell time is 0.6 ± 0.2 ms with a mean equivalent charge of 17.4 ± 3.1 fAs, which were calculated from the histogram fits, both values being in good agreement with previously reported data for 10 kbp DNA translocated from the external reservoir to the inside of the nanopipette.^{20,21}

Figure 2d illustrates single molecule delivery cycle reproducibility for two negative voltages of $V = -200$ mV and $V = -400$ mV, respectively. Five representative I-t traces are shown for both potentials with a non-stochastic ‘time of arrival’ of the first molecule in each cycle with the remainder of events showing expectedly stochastic behavior with the time between successive events being $\delta t \ll dT$. Figure 2e_i shows the number of molecules delivered per cycle for 24 consecutive cycles (500 s recording). The average number of molecules delivered per cycle was 17.7 ± 4.5 at $V = -400$ mV, 13.1 ± 3.3 molecules at $V = -300$ mV and 8.0 ± 3.0 molecules at $V = -200$ mV. Importantly, Fig. 2e_{ii} illustrates the non-stochastic delivery with a histogram of dT for each cycle showing the distribution of the time of the first event. The first molecule is delivered faster for higher V . For 10 kbp DNA with $t^+ = 6.4$ s and $V^+ = 500$ mV the time to the first event is $dT_{V^- = -400 \text{ mV}} = 3.0 \pm 0.5$ s, $dT_{V^- = -300 \text{ mV}} = 3.8 \pm 1.1$ s and $dT_{V^- = -200 \text{ mV}} = 6.1 \pm 0.9$ s. These results are not device-dependent as they have been reproduced with different nanopipettes.

Experiments analogues to the ones shown in Fig. 2 have been performed for 5 and 10 kbp DNA for a range of concentrations (3 pM to 1500 pM) and negative potentials V (-200 mV to -500 mV). Scatter plots and histograms showing delivery and detection of 5 kbp DNA molecules are available in Supplementary Fig. 1. Importantly, it was possible to reliably deliver and detect both 5 and 10 kbp DNA from concentrations as low as 3 pM (equal to 3 attomol of DNA sample in the nanopipette volume of 1 μ l), demonstrating the applicability of the method for the delivery and detection from ultra-small samples sizes without the need of amplification. These results indicate a detection sensitivity that is up to three orders of magnitude higher compared to the nanopipette literature^{8,18,20} and is directly comparable to ultra-low concentration detection (3.8 pM DNA) only accomplished with the usage of high salt gradients across the nanopore.⁴

Multiple single molecule delivery data has been summarized in the Supporting Information as measurements of 5 and 10 kbp DNA capture rates as a function of V at concentrations varying from 3 pM to 1500 pM (Supplementary Fig. 2).

The transport of DNA through the nanopipette can in the first instance be seen as interplay of electrophoretic (EP) and electroosmotic (EO) forces. During a V pulse, for the quartz nanopipettes used in our experiments, the electroosmotic flow is directed from the outside to the inside of the nanopipette, while EP pulls DNA molecules from the nanopipette interior to the outside. In a V^+ pulse the opposite occurs, the electroosmotic flow is directed out of the nanopipette, while EP pulls the DNA molecules further inside. Under negative (V^-) potentials DNA molecules are uncoiled and threaded inside the tip, and under positive (V^+) potential the DNA is pulled inside the nanopipette where it recoils. To estimate the rate of transport of DNA in the nanopipette, the following approximate expression is used:

$$C_R = \frac{\mu_{ep}I}{K}C + Q_{eo}C \quad (1)$$

where C_R is the average number of DNA molecules passing a cross-section of the nanopipette per second (equal to the average capture rate at the nanopipette tip), C is the concentration of DNA in the nanopipette, μ_{ep} is the electrophoretic mobility of the DNA, I is the ion current, K the (bulk) ion conductivity and Q_{eo} the electroosmotic flow. This expression is based on the assumption of having, on average, the same amount of DNA passing each cross section of the nanopipette. Even if the concentration of ions close to the tip of the nanopipette is expected to change under conditions of ion rectification, the concentration far from the tip should be independent of the sign of the applied voltage^{24,25} and the electric field in that region can then be estimated by I/K . The meaning of the terms in eq (1) close to the tip might be different, but does

not need to be considered to estimate C_R . Other forces such as dielectrophoresis might also act on the DNA close to the tip of the pipette at elevated voltages,²⁶ but this effect does not seem to dominate the transport of DNA in the present experiments and has thus been neglected from the analysis.

Finite element simulations were performed in COMSOL Multiphysics 4.3b to estimate I and Q_{eo} under different applied voltages (c.f. the Methods section and Supplementary Fig. 3) for the same nanopipette geometry as measured optically and by SEM. The time to the first event, dT , depends in this simplified model only on the three parameter V^+ , V^- and t^+ as:

$$dT = -\frac{(\mu_{ep}I_+ + KQ_{eo,+})}{(\mu_{ep}I_- + KQ_{eo,-})}t_+ \quad (2)$$

where the +/- signs indicate the ion current and the electroosmotic flow rate for the positive/negative pulses. Inserting the simulated values for the ion current and the electroosmotic flow (Supplementary Fig. 3b,c) gives dT as a function of V , V^+ and t^+ only. Figure 3a shows the values of dT predicted for different V (for $V^+ = 500$ mV and $t^+ = 6.4$ s), which are in excellent agreement with the experimental values consisting of 643 delivery cycles for 5 kbp and 10 kbp DNA molecules with a concentration of 30 pM and 150 pM. As seen in eq (2), dT should be independent of molecular length and concentration (for the parameter values used in this work), which also was confirmed by experiments for 5 kbp and 10 kbp DNA within a concentration range of 3 pM to 1500 pM (see Fig. 3a and Supplementary Fig. 4).

The number of DNA molecules delivered per pulse, N , is given by:

$$N = C_R(t^- - dT) \quad (3)$$

Together with eqs (1) and (2) it is thus observed that the number of molecules delivered in a negative pulse with a set duration t^- is proportional to the analyte concentration C and the number of delivered molecules can be controlled by varying dT and in turn, by varying V^- (see Fig. 3b), V^+ or t^+ . The latter is demonstrated by experimental and simulated data in Fig. 3b, which shows N at different values of V^- . Equations (2) and (3) also predict a linear relationship between dT and the positive pulse duration t^+ . This was confirmed experimentally where t^+ was varied in 340 delivery cycles for $V^+ = 500$ mV, $V^- = -300$ mV and $t^- = 21$ s (see Fig. 3c). The value of the slope of the experimental data is $dT/t^+ = 0.69 \pm 0.03$ which is in an excellent agreement with the theoretical predicted slope of $dT/t^+ = 0.71$. Both the theoretical and experimental results demonstrate that for a constant value of V^- the precise time of the delivery of the first molecule can be controlled by the duration of the positive potential t^+ . While molecular delivery occurs when negative pulses are applied, decreasing the duration of the positive pulse t^+ results in quicker delivery of the first molecule.

Additionally, for fixed values of V^- and t^- , the total number of delivered molecules per pulse is controlled by t^+ (see Fig. 3d). C_R is independent of t^+ and t^- (as measured experimentally and shown in the inset in Fig. 3d) and the only time dependence in N is thus in the term $(t^- - dT)$ (see eq (3)). Since dT is proportional to t^+ (as given by eq (2) and experimentally shown in Fig. 3c), the total number of delivered molecules varies linearly decrease with t^+ as shown both in the experimental and the simulated data in Fig. 3d.

Importantly, these findings confirm that during alternating pulses DNA molecules are transported back and forth close to the nanopipette tip and demonstrate that the potentials V^+ and V^- , as well as the pulse duration t^+ , can be used to actively control the delivery of a defined number of DNA molecules. The stochastic control over dT can further be used for precise

delivery of individual molecules in a single cycle. Based on eq (3) the negative pulse duration τ can be set such that on average only one molecule is delivered in a pulse (as shown in several consecutive cycles in Fig. 4a). The latter is also demonstrated in Fig. 4b_i to b_{iii} for three different combinations of τ^+ and τ (with up to 75 cycles each), chosen for values of dT such that $N = 1$ as predicted from eqs (2) and (3). Note, that since dT is proportional to τ^+ it is possible to deliver single molecules quickly in a short pulse with low dT , just by varying τ^+ (as can be seen from the pulse durations in Fig. 4b). Figure 4c_(i-iii) shows the distribution of the number of molecules delivered in a cycle for each of the τ^+ and τ combinations. Additional experimental data (plots of dT distribution and the number of molecules delivered per cycle) for a constant τ^+ (hence a constant dT), showing, as predicted, an increase of the number of delivered molecules per cycle with increasing τ , are available in Supplementary Fig. 5.

The control over dT can further be used to pulse molecules in the pipette tip close to the nanopore and back without delivering the molecule when in the regime $\tau < dT$. Molecular delivery can thus be switched on-demand for $\tau > dT$ (as shown in Fig. 4d) to deliver a specific number of molecules. In principle, the experimental regimes presented in Fig. 4a,d can be combined to alternate between pulsing a molecule in the tip and on-demand delivery of a single molecule.

The unique capabilities of on-demand, switchable molecular delivery and simultaneous label-free detection can be a particularly powerful tool in studies with living cells. The nanopipettes used in this work can be readily integrated with ion conductance microscopy to scan the surface of living cells and perform targeted delivery on demand in a cell area of choice. Another exciting application is using the nanopipette tip as an ultra-small reaction volume where small molecular populations are pulsed back and forth and interact with each other, with the reaction products simultaneously detected and delivered by the nanopore.

In this letter we showed controllable (non-stochastic) delivery of single DNA molecules with simultaneous label-free detection. We demonstrate that even highly diluted unamplified molecular populations can be precisely controlled and efficiently delivered with control of the time of delivery of the first molecule and number of delivered molecules in a single pulse. The latter can be readily implemented in scanning ion conductance microscopes for real-time imaging combined with targeted delivery inside living cells, thus creating the unique opportunity to control and study life processes such as gene regulation and infection quantitatively, one molecule at a time.

Methods

Nanopipette fabrication

Nanopipettes were fabricated using a P-2000 laser puller (Sutter Instrument Co,USA) from quartz capillaries with an outer diameter of 1 mm and an inner diameter of 0.50 mm (QF100-50-7.5; Sutter Instrument Co,USA).

Nanopipettes were fabricated using a two-lines protocol: 1) HEAT: 575; FIL: 3; VEL: 35; DEL: 145; PUL: 75, followed by 2) HEAT: 900; FIL: 2; VEL: 15; DEL: 128; PUL: 200. It should be noted that the pulling program is instrument specific and there is variation between P-2000 pullers.

Theoretical Modelling and Simulations

Finite element simulations were performed in COMSOL Multiphysics 4.3b to model the electric field, the ion current and the electroosmotic flow in a nanopipette with $R_0 = 12$ nm, $\theta = 3.5^\circ$ and $R_1 = 2R_0$. Similar simulations have previously been done for nanopores^{25 24} and for nanopipettes²⁷. The geometry used for the simulations is shown in Supplementary Fig. 3. The surface charge of the nanopipette walls, σ , was estimated for 0.1 M KCl (conductivity of $K \approx 1.5$ S/m) as:

$$\sigma = \kappa \epsilon_r \epsilon_0 \zeta \quad (4)$$

where κ is the inverse Debye length, I the ionic strength of the solution, ϵ_r the relative permittivity of the solution, ϵ_0 the permittivity of vacuum and ζ the zeta potential of the nanopipette walls. The zeta potential for glass in a 0.1 M K^+ solution is approximately -30 mV (see ref.²⁸) resulting in a surface charge of -22 mC/m². The simulated ion current through the

pore is of the same magnitude as the experimental values (as shown in Fig. 1d). The simulated curve also shows similar rectification ration $I_{-500 \text{ mV}} / I_{500 \text{ mV}} = 1.54$ compared to $I_{-500 \text{ mV}} / I_{500 \text{ mV}} = 1.64$ from the experiments.

To estimate the dwell time of the DNA being transported through the nanopore, we consider threading of a coil of DNA positioned a distance h from the tip of the nanopipette. The dwell time is then estimated as the total length of the DNA strand divided by the average velocity in the nanopipette in the range $0 < z < h$ (which is determined from the simulations as $v = \mu_{\text{ep}}E_z + v_{\text{eo}}$, where $\mu_{\text{ep}} = -4 \times 10^{-8} \text{ m}^2/\text{V s}$ is the electrophoretic mobility of DNA,²⁹ E_z is the electric field in the direction of the nanopipette axis and v_{eo} the electroosmotic velocity. $Q = \frac{\mu_{\text{ep}}I}{K} + Q_{\text{eo}}$

The velocity of the DNA at different positions, z , from the nanopore is given by:

$$v(z) = \frac{C_r/C}{\pi(R_0 + z \tan(\theta))^2} \quad (5)$$

Travelling a distance z from nanopore then takes $dz = v(z)dt$, hence

$$\pi \frac{(R_0 + z \tan(\theta))^3 - R_0^3}{3 \tan(\theta)} = \left(\frac{\mu_{\text{ep}}I}{K} + Q_{\text{eo}} \right) t \quad (6)$$

which for a positive pulse with duration t^+ followed by a negative pulse gives the expression in eq(2).

$$dT = - \frac{(\mu_{\text{ep}}I_+ + KQ_{\text{eo},+})}{(\mu_{\text{ep}}I_- + KQ_{\text{eo},-})} t_+$$

Measurement setup

The ion current was measured using a MultiClamp 700B or AxoPatch 200B patch-clamp amplifier (Molecular Devices, USA) in “voltage clamp” mode. The signal was filtered using a low-pass filter at 10 kHz and digitized with an Axon Digidata 1322A or Digidata 1440 at 50 kHz rate and recorded using pClamp 8/10 software (Molecular Devices, USA). Data analysis was carried out using a custom-written MATLAB analysis routine.

FIGURES

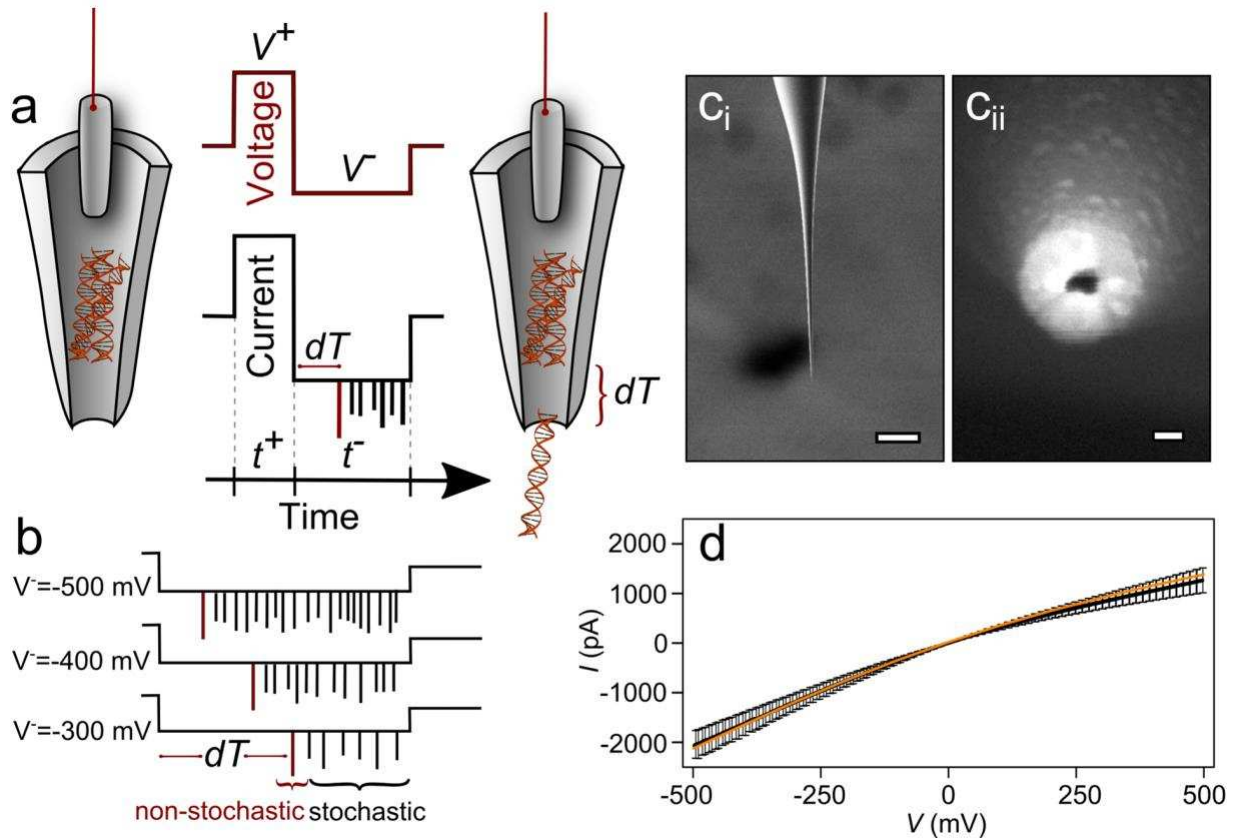


Figure 1 | Controlled delivery with nanopipette system. **a**, Schematic illustration showing the nanopipette delivery system. Positive (V^+) and negative (V^-) voltage pulses are applied for t^+ and t^- , respectively. **b**, Single DNA molecules are delivered during a (V) pulse and are detected as transient changes in the ion current. **c**, SEM images of the nanopipette tip (c_i) and the nanopore at the tip (c_{ii}). The scale bars are 250 μm and 25 nm, respectively. The nanopipettes had an inner half-cone angle of $\theta = 3.5^\circ$ resulting in a high length to width ratio of the nanopipette tip. **d**, Average I-V curves of 10 nanopipettes measured in 0.1 M KCl (black). The average ionic resistance was $R = 250 \pm 35$ M Ω . All nanopipettes exhibited ion current rectification with a ratio $I_{-500 \text{ mV}}/I_{500 \text{ mV}} = 1.64 \pm 0.40$. The orange line is an I-V curve calculated by finite element simulations in COMSOL Multiphysics by modeling the electric field, ion current and

electroosmotic flow in the nanopipette as described in the Methods section. The simulated rectification ratio is $I_{-500 \text{ mV}} / I_{500 \text{ mV}} = 1.54$.

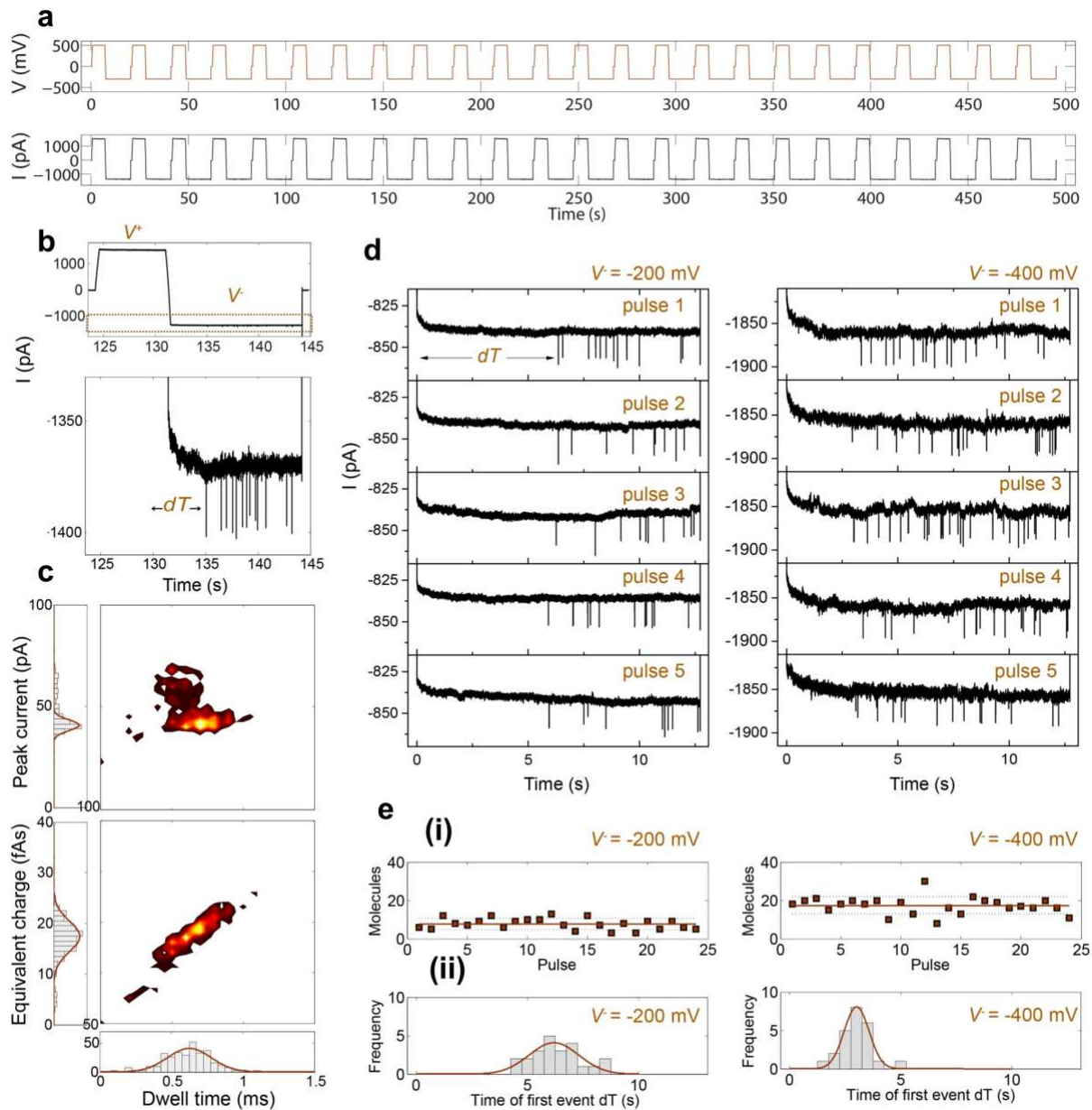


Figure 2 | Single molecule detection and delivery. **a**, I-t and V-t measurements of the first 500 s (24 delivery cycles) of 150 pM, 10 kbp DNA, with $V^+ = 500$ mV, $V^- = -300$ mV, $t^+ = 6.4$ s and $t^- = 12.7$ s. **b**, A single voltage cycle and a blow up of individual delivery events. **c**, Event scatter plots of peak current versus dwell time (top panel) and equivalent charge vs dwell time (bottom panel) for the 24 cycles show in **a**. At $V^- = -300$ mV the most probable pore dwell time

is 0.65 ± 0.21 ms with a mean charge (integrated current area per translocation) of 18.0 ± 4.1 fAs, as calculated from the histogram fits. **d**, Representative I-t traces for delivery of 150 pM, 10 kbp DNA for $V = -200$ mV and $V = -400$ mV. **e_i**, Data points showing the number of delivered DNA molecules per cycle. The orange solid line shows the average number of molecules delivered per cycle: 17.7 ± 4.5 molecules at $V = -400$ mV, 13.1 ± 3.3 molecules at $V = -300$ mV and 8.0 ± 3.0 molecules at $V = -200$ mV. **e_{ii}**, Histogram showing the time distribution of the first event in a delivery cycle for the 24 delivery cycles. The first molecule is delivered faster for higher V

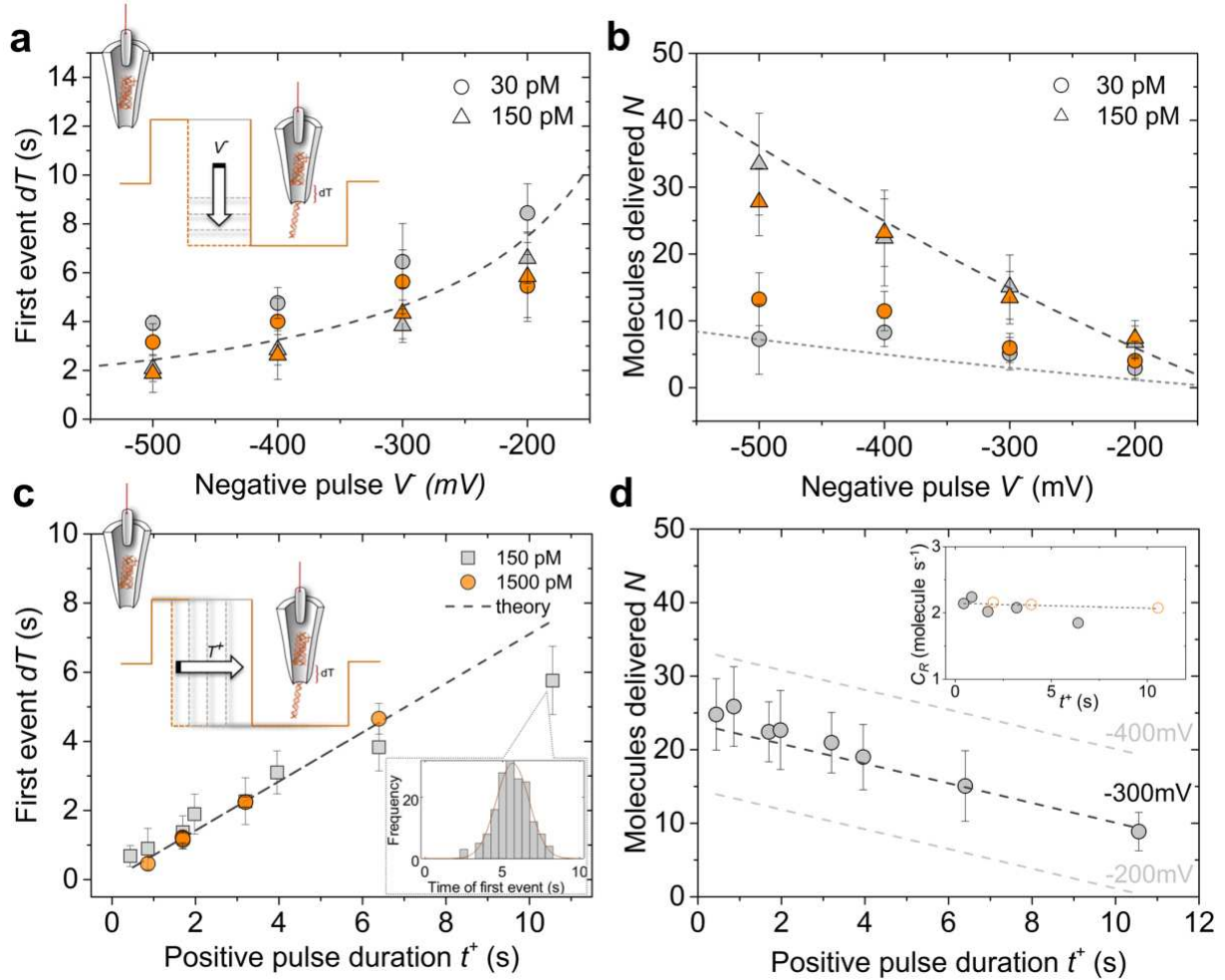


Figure 3 | Non-stochastic delivery of molecules. The time of the first event dT and the number of molecules delivered in a pulse is precisely controlled by the potentials V^+ and V^- and the positive pulse duration t^+ . **a**, Experimentally measured time of the first event as a function of the applied potential V^- for 356 delivery cycles of 10 kbp DNA (gray) and 5 kbp DNA (orange), and predicted values of dT from eq (2) (dashed line). Both experiments and simulations have been carried out for positive pulses, $V^+ = 500$ mV and $t^+ = 6.4$ s. **b**, Number of molecules N delivered in a set negative pulse ($t^- = 12.7$ s) for different negative pulse potentials V^- for 10 kbp DNA (gray) and 5 kbp DNA (orange), and predicted values of dT from eq (3) (dashed lines). **c**, Time of the first event as a function of t^+ for 150 pM (gray) and 1500 pM (orange), 10 kbp DNA, with $V^+ = 500$ mV and $V^- = -300$ mV. The dashed line shows the predicted values of dT

from eq (2). The inset shows a histogram of 168 dT measurements for $t^+ = 10.6$ s, exhibiting a normal distribution. A total number of 5501 DNA molecules were delivered over 5700 s. **d**, Number of delivered molecules per pulse ($t = 12.7$ s) for different positive pulse duration t^+ ($V^+ = 500$ mV and $V = -300$ mV). (inset) DNA capture rate measurements for different positive pulse durations t^+ for $t = 12.7$ s (\circ) and $t = 21.0$ s (\bullet). The dashed lines are theoretical values from eqs (2) and (3).

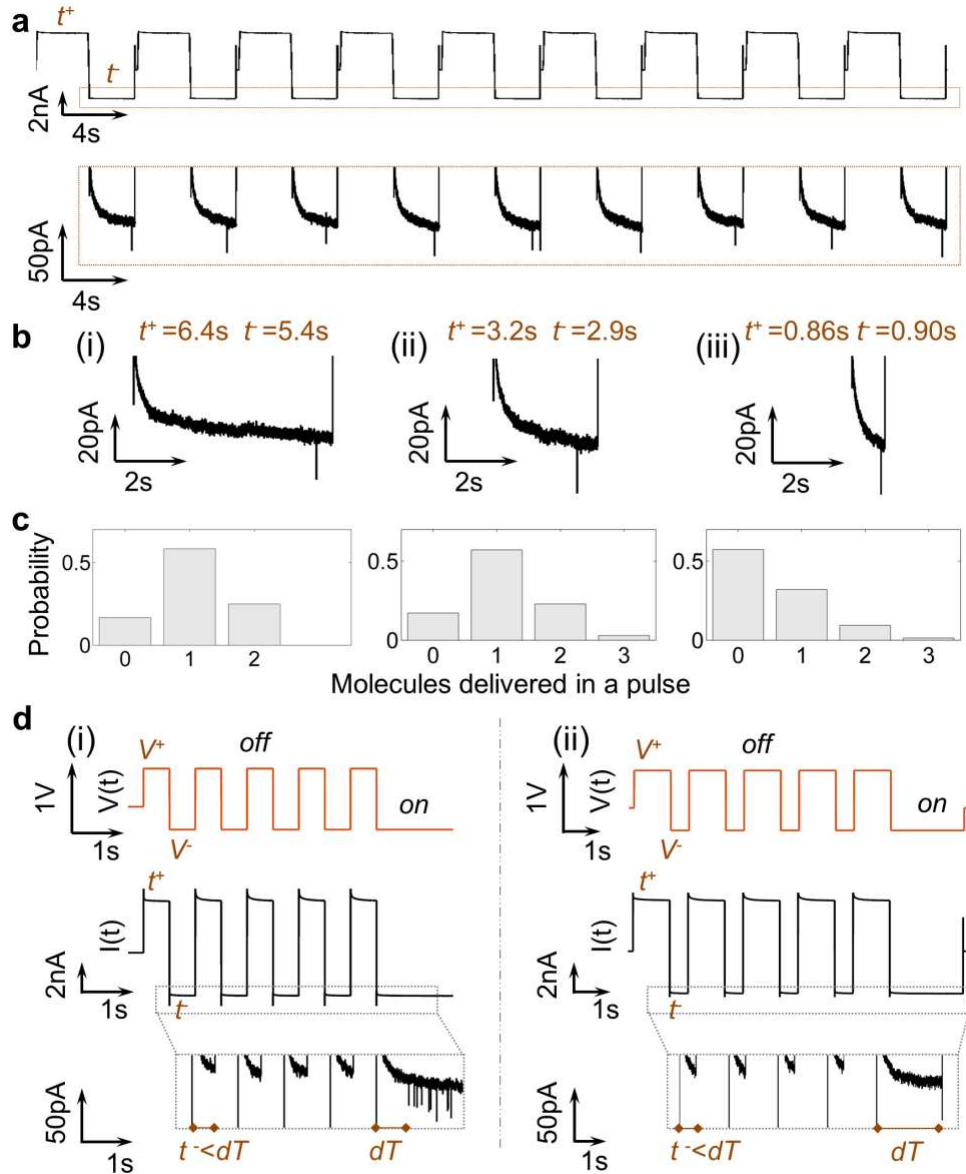


Figure 4 | Delivery of individual molecules in single pulses. **a**, I-t trace showing nine consecutive cycles delivering a single molecule per pulse (top panel) and blow up of the single events (lower panel) for 1500 pM, 10 kbp DNA with $V^+ = 500\text{ mV}$, $V^- = -300\text{ mV}$, $t^+ = 3.2\text{ s}$ and $t^- = 2.9\text{ s}$. **b**, Representative I-t pulses for different t^+ and t^- combinations. dT is proportional to t^+ hence single molecules are delivered quicker by varying t^+ in a short pulse. **c**, Distribution of the number of molecules delivered in a cycle for each t^+ and t^- combination shown in **b**.

d, Delivery on demand. Graphs showing the applied voltage pulses and the recorded ion current for different negative pulse lengths for 1500 pM, 10kbp DNA with $V^+ = 500$ mV and $V^- = -300$ mV. By using an asymmetric nanopore geometry and square wave voltage pulses, molecules can be pulsed in the nanopipette tip close to the nanopore and back without being delivered when operated in the regime $\tau < dT$. Molecular delivery can be switched on-demand for $\tau > dT$. $\tau = 15$ s

References

- 1 Dekker, C. Solid-state nanopores. *Nat Nanotechnol* **2**, 209-215, doi:10.1038/Nnano.2007.27 (2007).
- 2 Venkatesan, B. M. & Bashir, R. Nanopore sensors for nucleic acid analysis. *Nat Nanotechnol* **6**, 615-624, doi:Doi 10.1038/Nnano.2011.129 (2011).
- 3 Miles, B. N. *et al.* Single molecule sensing with solid-state nanopores: novel materials, methods, and applications. *Chemical Society reviews* **42**, 15-28, doi:10.1039/c2cs35286a (2013).
- 4 Wanunu, M., Morrison, W., Rabin, Y., Grosberg, A. Y. & Meller, A. Electrostatic focusing of unlabelled DNA into nanoscale pores using a salt gradient. *Nat Nanotechnol* **5**, 160-165, doi:Doi 10.1038/Nnano.2009.379 (2010).
- 5 Ivanov, A. P. *et al.* DNA Tunneling Detector Embedded in a Nanopore. *Nano Lett* **11**, 279-285, doi:10.1021/nl103873a (2010).
- 6 Wei, R., Gatterdam, V., Wieneke, R., Tampe, R. & Rant, U. Stochastic sensing of proteins with receptor-modified solid-state nanopores. *Nat Nanotechnol* **7**, 257-263, doi:10.1038/nnano.2012.24 (2012).
- 7 Karhanek, M., Kemp, J. T., Pourmand, N., Davis, R. W. & Webb, C. D. Single DNA Molecule Detection Using Nanopipettes and Nanoparticles. *Nano Lett* **5**, 403-407, doi:10.1021/nl0480464 (2005).
- 8 Steinbock, L. J., Otto, O., Chimere, C., Gornall, J. & Keyser, U. F. Detecting DNA Folding with Nanocapillaries. *Nano Lett* **10**, 2493-2497, doi:10.1021/nl100997s (2010).
- 9 Li, W. *et al.* Single Protein Molecule Detection by Glass Nanopores. *Acs Nano* **7**, 4129-4134, doi:10.1021/nm4004567 (2013).
- 10 Novak, P. *et al.* Nanoscale live-cell imaging using hopping probe ion conductance microscopy. *Nat Methods* **6**, 279-281, doi:Doi 10.1038/Nmeth.1306 (2009).
- 11 Actis, P. *et al.* Electrochemical Nanoprobes for Single-Cell Analysis. *Acs Nano* **8**, 875-884, doi:Doi 10.1021/Nn405612q (2014).
- 12 Knoblauch, M., Hibberd, J. M., Gray, J. C. & van Bel, A. J. E. A galinstan expansion femtosyringe for microinjection of eukaryotic organelles and prokaryotes. *Nat Biotechnol* **17**, 906-909, doi:Doi 10.1038/12902 (1999).
- 13 Bruckbauer, A. *et al.* Nanopipette delivery of individual molecules to cellular compartments for single-molecule fluorescence tracking. *Biophys J* **93**, 3120-3131, doi:DOI 10.1529/biophysj.107.104737 (2007).
- 14 Singhal, R. *et al.* Multifunctional carbon-nanotube cellular endoscopes. *Nat Nanotechnol* **6**, 57-64, doi:Doi 10.1038/Nnano.2010.241 (2011).
- 15 Adam Seger, R. *et al.* Voltage controlled nano-injection system for single-cell surgery. *Nanoscale* **4**, 5843-5846 (2012).
- 16 Babakinejad, B. *et al.* Local Delivery of Molecules from a Nanopipette for Quantitative Receptor Mapping on Live Cells. *Analytical chemistry* **85**, 9333-9342, doi:10.1021/ac4021769 (2013).
- 17 Ying, L., Bruckbauer, A., Rothery, A. M., Korchev, Y. E. & Klenerman, D. Programmable Delivery of DNA through a Nanopipet. *Analytical chemistry* **74**, 1380-1385, doi:10.1021/ac015674m (2002).

- 18 Steinbock, L. J., Lucas, A., Otto, O. & Keyser, U. F. Voltage-driven transport of ions and DNA through nanocapillaries. *Electrophoresis* **33**, 3480-3487, doi:10.1002/elps.201100663 (2012).
- 19 Bell, N. A. *et al.* Multiplexed ionic current sensing with glass nanopores. *Lab on a chip* **13**, 1859-1862, doi:10.1039/c3lc50069a (2013).
- 20 Gong, X. *et al.* Label-free in-flow detection of single DNA molecules using glass nanopipettes. *Analytical chemistry* **86**, 835-841, doi:10.1021/ac403391q (2014).
- 21 Gibb, T. R., Ivanov, A. P., Edel, J. B. & Albrecht, T. Single Molecule Ionic Current Sensing in Segmented Flow Microfluidics. *Analytical chemistry* **86**, 1864-1871, doi:10.1021/ac403921m (2014).
- 22 Lan, W.-J., Holden, D. A. & White, H. S. Pressure-Dependent Ion Current Rectification in Conical-Shaped Glass Nanopores. *J Am Chem Soc* **133**, 13300-13303, doi:10.1021/ja205773a (2011).
- 23 Smeets, R. M. M. *et al.* Salt Dependence of Ion Transport and DNA Translocation through Solid-State Nanopores. *Nano Lett* **6**, 89-95, doi:10.1021/nl052107w (2005).
- 24 Kubeil, C. & Bund, A. The Role of Nanopore Geometry for the Rectification of Ionic Currents. *Journal of Physical Chemistry C* **115**, 7866-7873, doi:10.1021/Jp111377h (2011).
- 25 White, H. S. & Bund, A. Ion current rectification at nanopores in glass membranes. *Langmuir* **24**, 2212-2218, doi:Doi 10.1021/La702955k (2008).
- 26 Ying, L. *et al.* Frequency and voltage dependence of the dielectrophoretic trapping of short lengths of DNA and dCTP in a nanopipette. *Biophys J* **86**, 1018-1027, doi:10.1016/S0006-3495(04)74177-6 (2004).
- 27 Sa, N. & Baker, L. A. Experiment and Simulation of Ion Transport through Nanopipettes of Well-Defined Conical Geometry. *Journal of the Electrochemical Society* **160**, H376-H381, doi:10.1149/2.128306jes (2013).
- 28 Kirby, B. J. & Hasselbrink, E. F., Jr. Zeta potential of microfluidic substrates: 1. Theory, experimental techniques, and effects on separations. *Electrophoresis* **25**, 187-202, doi:10.1002/elps.200305754 (2004).
- 29 Nkodo, A. E. *et al.* Diffusion coefficient of DNA molecules during free solution electrophoresis. *Electrophoresis* **22**, 2424-2432, doi:10.1002/1522-2683(200107)22:12<2424::AID-ELPS2424>3.0.CO;2-1 (2001).